International Immunopharmacology 136 (2024) 112377

Contents lists available at ScienceDirect

International Immunopharmacology

journal homepage: www.elsevier.com/locate/intimp

CDDP-induced desmoplasia-like changes in oral cancer tissues are related to SASP-related factors induced by the senescence of cancer cells

Junya Nishimura, Yoshihiro Morita *, Ayano Tobe-Nishimoto, Yukiko Kitahira, Shun Takayama, Satoko Kishimoto, Yuka Matsumiya-Matsumoto, Akinori Takeshita, Kazuhide Matsunaga, Tomoaki Imai, Narikazu Uzawa

Department of Oral & Maxillofacial Oncology and Surgery, Osaka University Graduate School of Dentistry, Suita-shi, Osaka 565-0871, Japan

ARTICLE INFO

Keywords:
Oral cancer
Tumor microenvironment
Desmoplasia-like change
Senescence
Chemotherapy

ABSTRACT

The tumor microenvironment (TME) concept has been proposed and is currently being actively studied. The development of extracellular matrix (ECM) in the TME is known as desmoplasia and is observed in many solid tumors. It has also been strongly associated with poor prognosis and resistance to drug therapy. Recently, cellular senescence has gained attention as an effect of drug therapy on cancer cells. Cellular senescence is a phenomenon wherein proliferating cells become resistant to growth-promoting stimuli, secrete the SASP (senescence-associated phenotypic) factors, and stably arrest the cell cycle. These proteins are rich in pro-inflammatory factors, such as interleukin (IL)-6, IL-8, C-X-C motif chemokine ligand 1, C–C motif chemokine ligand (CCL)2, CCL5, and matrix metalloproteinase 3. This study aimed to investigate the desmoplasia-like changes in the TME before and after cancer drug therapy in oral squamous cell carcinomas, evaluate the effect of anticancer drugs on the TME, and the potential involvement of cancer cell senescence. Using a syngeneic oral cancer transplant mouse model, we confirmed that *cis*-diamminedichloroplatinum (II) (CDDP) administration caused desmoplasia-like changes in cancer tissues. Furthermore, CDDP treatment-induced senescence in tumor-bearing mouse tumor tissues and cultured cancer cells. These results suggest CDDP administration-induced desmoplasia-like structural changes in the TME are related to cellular senescence. Our findings suggest that the administration of anticancer drugs alters the TME of oral cancer cells. Additionally, oral cancer cells undergo senescence, which may influence the TME through the production of SASP factors.

1. Introduction

In recent years, substantial changes have been made to cancer research. Malignant tumor cells have long been the object of study, and investigations have focused on analyzing the processes leading to their transformation and changes in malignant potential. However, such changes in malignant tumor cells involve a group of non-tumor cells around the malignant tumor [1]. Therefore, the concept of the tumor microenvironment (TME), which views the tumor as a complex structure that includes tumor cells and the surrounding cell population, has been proposed and is currently under active research. The individual components of TME are increasingly becoming the focus of cancer research. These studies have been utilized to develop drugs targeting the TME and their clinical applications, starting with angiogenesis inhibitors and introducing immunotherapeutics with the potential to disrupt the status quo [2,3].

The extracellular matrix (ECM) is a component of TME that initially received the least attention. However, our understanding of the role of ECM in malignant tumors and the changes in ECM concerning therapy has been enhanced by numerous studies [1]. In many solid tumors, the tumor cells express high molecules comprising various ECM components, including fibrous collagen, fibronectin, elastin, and laminin [4,5]. The ECM accounts for approximately 60 % of the total volume of tumor tissue and comprises tumor cells, tumor-associated fibroblasts (CAFs), and tumor-associated macrophages (TAMs), which are components of the TME. Macrophages (TAMs) are involved in ECM formation [6–9]. ECM formation, specifically fibrosis of tumor tissue resulting from the accumulation of fibrous collagen and other substances, is termed

* Corresponding author at: Department of Oral & Maxillofacial Oncology and Surgery, Osaka University Graduate School of Dentistry, 1-8 Yamadaoka, Suita-shi, Osaka 565-0871, Japan.
E-mail address: morita.yoshihiro.dent@osaka-u.ac.jp (Y. Morita).

https://doi.org/10.1016/j.intimp.2024.112377
Received 28 February 2024; Received in revised form 10 May 2024; Accepted 28 May 2024
Available online 4 June 2024

desmoplasia, has been observed in many solid tumors, and has been reported to be strongly associated with poor prognosis and resistance to drug therapy [1,10,11].

In addition, anticancer treatments have been reported to induce inflammation [12,13]. Guthrie et al. reported that cancer-associated inflammation is a key determinant for treatment outcomes in patients with cancer. Correlative studies (15 studies, >8,500 patients) have shown elevated inflammation in patients with advanced or aggressive disease, indicated by increased tumor stage, nodal stage, and number of metastatic lesions. These patients may represent a particularly high-risk population. Moreover, Schaue et al. reported that the immune system can modulate the expression of radiation-induced normal and tumor tissue damage. It can contribute to cancer cure while also influencing acute and late radiation side effects, which resemble acute and chronic inflammatory disease states.

Recently, cellular senescence has gained attention as an effect of drug therapy on cancer cells. Cells are considered to undergo senescence when proliferating cells resist growth-promoting stimuli and stably arrest the cell cycle, as observed in the DNA damage response. In drug and radiation therapy for cancer, sufficient doses of anticancer drugs and radiation induce apoptosis in cancer cells, leading to cell death [14,15]. In contrast, anticancer drugs and radiation to a nonlethal degree to cancer cells have been reported to induce senescence in cancer cells [14,15]. Although the long-term survival mechanisms of residual cancer cells after drug therapy remain poorly understood, recent studies have shown that the senescence of cancer cells contributes to cancer recurrence [16–18]. Two pathways are known the induce senescence via the cell cycle regulators, p21 and p16, the expression of which is upregulated, leading to cell cycle arrest [19]. In addition, senescent cancer cells, such as normal senescent cells, have been recently reported to acquire a phenotype called the senescence-associated secretory phenotype (SASP), which is the result of a persistent DNA damage response associated with the inflammatory SASP. It is a proinflammatory phenotype that results from a sustained DNA damage response and increases the expression of genes encoding secreted proteins such as cytokines [20]. These secreted proteins are rich in proinflammatory factors, such as interleukin (IL)-6, IL-8, C-X-C motif chemokine ligand (CXCL)1, C–C motif chemokine ligand (CCL)2, CCL5, and matrix metalloproteinase (MMP)3 [21,22]. These SASP factors are secreted after cellular senescence, which may cause cancer recurrence by stimulating surrounding non-aging breast cancer cells in breast cancer tissue [22,23].

Oral cancer is the 18th most common malignancy among 36 sites [24]. According to Japanese Cancer Statistics, more than 22,000 patients in Japan were affected by lip and oral cavity cancer and pharyngeal cancer in 2018 [24]. Approximately 90 % of oral cancers are oral squamous cell carcinomas (OSCC) [25], which generally occur at the lateral border of the tongue and upper and lower gingiva, and their treatment markedly reduces oral function and quality of life [24,26,27]. In oral cancer, platinum-based drug therapy, including *cis*-diamminedichloroplatinum (II) (CDDP), has been indicated for locally advanced cases and recurrent metastases. However, no reports have been found in examining desmoplasia-like changes after drug therapy for oral cancer. Hence, the relationship between senescence and desmoplasia in oral cancer cells remains unclear [28].

In this study, we aimed to examine desmoplasia-like changes within the TME before and after cancer drug therapy in OSCC, evaluate the effect of anticancer drugs on the TME, and determine the potential involvement of cancer cell senescence in this process.

2. Materials and methods

2.1. Clinical samples

The subjects were seven patients with oral cancer treated with neoadjuvant drug therapy, including CDDP, in our department between 2011 and 2019, in whom biopsy and surgical resection of clinicopathological specimens allowed comparison of histopathology before and after drug therapy (Table 1). Picrosirius Red staining was performed to evaluate the thickness and amount of collagen in the tumor tissue before and after drug therapy. Picrosirius Red staining was performed to evaluate the thickness and amount of collagen in the tumor tissue before and after drug therapy. The TNM classification and therapeutic effects are based on the Oral Cancer Treatment Regulations (2nd edition) [29]. The study protocol was approved by the Institutional Review Board of the Graduate School of Dentistry, Osaka University.

2.2. Cell preparation and culture

NR-S1 cells, a cell line derived from mouse oral squamous cell carcinoma, were used in the experiments [30]. Cells were grown in Dulbecco's medium containing 10 % fetal bovine serum (FBS: Equitech-Bio Inc, Kerrville, TX, USA) and 100 μg/mL kanamycin (Meiji Seika Pharma Co., Ltd., Tokyo, Japan) under 37 °C, 5 % CO2 vapor phase. The experiments were performed in Dulbecco's modified Eagle's medium (DMEM) and Ham's/F^2 medium (D-MEM Ham's/F^2: FUJIFILM Wako Pure Chemicals Corporation, Osaka, Japan). The experiments were performed under the following conditions:

2.3. Mouse models and drug administration

All animal experiments were reviewed and approved by the Animal Experiment Committee of the Graduate School of Dentistry, Osaka University. Five to 6-week-old male C3H mice (SLC, Shizuoka, Japan) were treated with midazolam (4.0 mg/kg body weight, Dormicum®: Astellas Pharma Inc). NR-S1 cells (1×10^6/100 μL) were suspended in cell culture medium, and 100 μL were inoculated at the center of the tongue apex. One hundred microliters were inoculated into the center of the apex of the tongue. After confirming tumor formation and growth, CDDP (cisplatin injection 10 mg, Nichi-Iko Corporation, Toyama, Japan) was administered at a concentration of 10 mg/20 mL twice a week at 200 μL each time via the tail vein or p21 inhibitor UC2288 (Selleck Biotech, Tokyo, Japan) was administered at a concentration of 2.5 mg/mL twice a week at 50 μL each time intraperitoneally. The control group received a saline solution or dimethyl sulfoxide (DMSO) during the same period. The tumors were removed three days after the final dose.

2.4. Immunohistochemistry

Clinical specimens and mouse tongue tumor tissues were subjected to immunohistological analysis. Mouse tongue tumor tissues were paraffin-embedded, cut into 4-μm-thick slices, and stretched on glass slides. After deparaffinization with xylene, tissues were hydrated with ethanol. Antigen activation was performed under pressure by boiling 1 mmol/L of ethylenediamine tetraacetic acid buffer (pH 8.0; NIPPON GENE Inc., Tokyo, Japan). A 3 % hydrogen peroxide solution was applied for 15 min to remove endogenous peroxidase, and 1 % bovine

Table 1
The list of clinicopathologic parameters for the clinical samples.

Age	Gender	Region	Diagnosis	TNM	Therapeutic Effect
62	Female	tongue	scc	T4aN0M0	Grade3
58	Female	tongue	scc	T2N1M0	Grade2
71	Male	maxilla	scc	T3N1M0	unknown
56	Male	maxillary sinus	scc	T3N1M0	Grade2
68	Male	maxillary sinus	scc	T2N0M0	Grade2
73	Male	maxillary sinus	scc	T2N1M0	Grade1
71	Male	buccal mucosa	scc	T4N0M0	Grade2

serum albumin was used for 60 min for blocking. Primary antibodies were allowed to react for 12 h at 4 °C (Table 2). Subsequently, mouse tissues were treated with Histofine Simple Stain Mouse MAX-PO(R) (Nichirei Bioscience, Tokyo, Japan), an anti-rabbit IgG antibody. In contrast, human tissues were treated with Histofine Simple Stain MAX-PO(MULTI) (Nichirei Bioscience, Tokyo, Japan), an anti-rabbit IgG antibody. Tokyo, Japan) and visualized using the peroxidase substrate ImmPACT NovaRED (Vector Laboratories Inc., California, USA).

Mouse tongue tumor tissue sections were stained, and five fields of view with the most positive areas were photographed under a microscope (Leica DM IL LED; Leica Microsystems GmbH, Wetzlar, Germany) at 400x magnification. The percentage of positive areas per image was calculated using ImageJ image processing software (National Institutes of Health, USA).

2.5. Picrosirius Red Stain

Picrosirius red staining is commonly used as a histological technique to visualize collagen fibers in paraffin-embedded tissue sections [31]. Clinical specimens and paraffin sections of mouse tongue tumor tissues were deparaffinized with xylene, hydrated with ethanol, and treated with picrosirius red solution (ScyTek Laboratories, UT, USA) for 1 h. A 0.5 % Acetic Acid Solution (ScyTek Laboratories, UT, USA) was added 2 times and finally sealed with a MOUNT-QUICK (Dyu Sangyo Co. Ltd., Tokyo, Japan).

After staining, clinical specimens and mouse tongue tumor tissue were stained at 200x, and their surroundings, including the tumor parenchyma, were randomly photographed in five views under a polarized light microscope (Leica DM IL LED with polarizing filter; Leica Microsystems GmbH). ImageJ software was used to evaluate the positive areas, where thick collagen fibers depicted as yellow to orange were defined as positive areas, and the percentage of these areas per image was calculated.

2.6. CDDP treatment of oral cancer cells

The NR-S1 cell line was cultured to 50–70 % confluency in six-well dishes, and 20 μM CDDP was added to the culture medium and treated for 6 h. CDDP was removed, and the RNA was recovered after culturing in a standard culture medium with an incubation time of 24 h.

To prepare for cell immunostaining, the NR-S1 cell line was cultured in a 12-well chamber, removed for approximately 24 h, treated with 20 μM CDDP for 6 h, removed, and cultured in a standard culture medium for 24 h.

2.7. Inhibition of p21 using UC2288

The NR-S1 cell line was cultured to 50–70 % confluency in six-well dishes and treated with 20 μM CDDP only, and 20 μM CDDP plus 10 μM p21 inhibitor UC2288 (Selleck Biotech) diluted with DMSO in the medium was prepared and treated for 6 h each. The supernatant was removed, and RNA was collected after 24 h of incubation in a normal culture medium.

Table 2
The list of antibodies used for immunocytochemistry and immunohistochemistry.

Antibody	Dilution	Company
p21	ICC (1:200) , IHC (1:300)	Bioss
CD45	IHC (1:200)	Cell signaling
F4/80	IHC (1:250)	Cell signaling
CD163	IHC (1:500)	Abcam

2.8. Immunofluorescence analysis

To prepare for cell immunostaining, the NR-S1 cell line was cultured in a 12-well-chamber, removable for approximately 24 h, and the medium was supplemented with 20 μM CDDP only and 20 μM CDDP plus 10 μM of the p21 inhibitor UC2288 diluted in DMSO, and each was treated for 6 h. The supernatant was removed, and the cells were incubated in a normal culture medium for 24 h, after which immunocytochemistry was performed.

2.9. RNA isolation and RT-qPCR

Reverse transcription-quantitative polymerase chain reaction (RT-qPCR) was performed using the following method. RNA was extracted from the cultured cells and tissues using a total RNA isolation system (Monarch Total RNA Miniprep Kit; New England Biolabs, MA, USA). First-strand cDNAs were synthesized using the ReverTraAce® qPCR RT Master Mix (Toyobo Co., Ltd., Osaka, Japan). Quantitative real-time PCR (qPCR) was performed using the SYBR Green PCR protocol and the StepOnePlus real-time PCR system (Applied Biosystems, Foster City, CA, USA) with n = 3 per sample. The SYBR Green primers used for amplification are listed in Table 3.

2.10. Statistical analysis

Experimental outcome data are presented as mean ± SD for in vitro and mean ± SEM for in vivo experiments. Comparisons between two independent groups were evaluated using Student's *t*-test, comparisons between two related groups using the paired *t*-test, 2 × 2 contingency table tests using Fisher's exact probability test, and comparisons between three groups using one-way analysis of variance (ANOVA) and Dunnett's multiple comparison test. Comparisons among the three groups were performed using one-way ANOVA and Dunnett's multiple comparison test. Statistical analyses were performed using the Prism 9 software (GraphPad Software, La Jolla, CA, USA). P-values less than 0.05 were considered statistically significant.

3. Results

3.1. Microenvironmental changes in clinical specimens before and after CDDP administration

Biopsy specimens before and after administering anticancer drugs were analyzed using Picro-Sirius Red staining, which specifically stains muscle and collagen fibers. Under a bright-field microscope, the bundling of collagen fibers was observed in the specimens after

Table 3
The list of SYBR Green primers used for amplification.

Gene name		Sequence (5′ → 3′)
p21	Forward	CCTGGTGATGTCCGACCTG
	Reverse	CCATGAGCGCATCGCAATC
p16-INK4a	Forward	CGCAGGTTCTTGGTCACTGT
	Reverse	TGTTCACGAAAGCCAGAGCG
IL-6	Forward	CCTGAGACTCAAGCAGAAATGG
	Reverse	AGAAGGAAGGTCGGCTTCAGT
CXCL1	Forward	ACTGCACCCAAACCGAAGTC
	Reverse	TGGGGACACCTTTTAGCATCTT
CXCL2	Forward	CCAACCACCAGGCTACAGG
	Reverse	GCGTCACACTCAAGCTCTG
CCL2	Forward	TTAAAAACCTGGATCGGAACCAA
	Reverse	GCATTAGCTTCAGATTTACGGGT
CCL5	Forward	GCTGCTTTGCCTACCTCTCC
	Reverse	TCGAGTGACAAACACGACTGC
CXCL9	Forward	TCCTTTTGGGCATCATCTTCC
	Reverse	TTTGTAGTGGATCGTGCCTCG
IL-13	Forward	CCTGGCTCTTGCTTGCCTT
	Reverse	GGTCTTGTGTGATGTTGCTCA

administration of the anticancer drug. Furthermore, under polarized light microscopy, bundled thick collagen fibers appeared yellow to orange in color, and the number of dense collagen fibers significantly increased after anticancer drug administration compared to that before anticancer drug administration (Fig. 1).

3.2. Microenvironmental changes induced by CDDP administration to tongue tumor tissues of tumor-bearing mice

Tongue tumors removed from tumor-bearing mice were evaluated using Picrosirius Red staining and immunohistochemistry. Picrosirius Red staining assessed the collagen fibers, as in the clinical specimens. Bundles of collagen fibers were observed in the CDDP-treated group by bright-field microscopy (Fig. 2A). Polarized light microscopy revealed that thick collagen fibers, depicted in yellow to orange, significantly increased in the CDDP-treated group compared to those in the control group (Fig. 2B). Furthermore, these CDDP-treated tumors showed clear tumor shrinkage compared to the control group (Supplementary Figure 1).

The number of total leukocytes positive for CD45 was significantly higher in the CDDP-treated group than in the control group (Fig. 2C). Similarly, CD163-positive M2 macrophages (M2-TAMs) significantly increased in the CDDP-treated group compared to those in the control group; however, TAMs were localized to tumor cells and infiltrated into tumor cells, whereas M2-TAMs showed little infiltration into tumor cells (Fig. 2C). These results indicate that CDDP administration induces desmoplasia-like structural changes in TME and inflammation with immune cell infiltration, which may be related.

3.3. Tongue tumor tissues of tumor-bearing mice and senescence of OSCC cells with increased p21 expression upon CDDP treatment

As mentioned above, the senescence of tumor cells induced by cancer drug therapy has recently attracted much attention [16]. Therefore, we evaluated the expression of p16 and p21, cell cycle regulators known as cellular senescence markers, using RNA extracted from mouse tongue tumors and RT-qPCR to confirm whether CDDP treatment induces senescence in tumor cells. p21 expression was significantly upregulated in the CDDP-treated group compared to that in the control group (Fig. 3A). However, no significant difference was observed for p16 between the two groups (Fig. 3A).

Next, NR-S1 cells (a mouse OSCC cell line) were treated with CDDP. The results showed that CDDP treatment increased the expression of p53 and p21 at the mRNA level (Fig. 3B). In contrast, the p16 expression was not detected in both groups (data not shown). To examine changes in p21 protein expression, immunocytochemistry was performed using NR-S1 cells 24 h after CDDP treatment. The results showed a higher expression of p21 in the nucleus and cytoplasm of CDDP-treated cells than in the controls (Fig. 3C).

3.4. Altered expression of SASP factors and other factors upon CDDP treatment of OSCC cell lines

Next, we analyzed the mRNA expression of representative SASP factors reported in the literature, IL-6, CXCL1, CXCL2, CCL2, CCL5, CXCL9, and IL-13, following CDDP treatment [32]. CCL2 is an SASP factor that regulates the migration and infiltration of various immune cells, including monocytes and macrophages [33]. The qPCR results showed that the expression levels of all SASP factors after 24 h of CDDP treatment were significantly upregulated compared with those in the control group (Fig. 4). The increased expression of typical SASP factors corroborates CDDP-induced senescence of cancer cells.

3.5. Altered expression of senescence markers and SASP factors in OSCC cell lines treated with CDDP and p21 inhibitor

To confirm that the senescence induced by CDDP treatment in OSCC cell lines is a p21-mediated phenomenon, we added UC2288, a p21 inhibitor, to CDDP-treated NR-S1 cells. p21 mRNA expression was significantly reduced by the addition of UC2288, confirming that p21 expression was inhibited by UC 2288, ensuring that p21 expression was inhibited by UC2288 (Fig. 5A). Furthermore, immunostaining analysis at the protein level showed decreased p21 expression in cells treated with CDDP and UC2288 compared to cells treated with CDDP alone (Fig. 5B).

Subsequently, to examine whether the increased expression of SASP factors by CDDP treatment of the OSCC cell lines was due to the senescence of cancer cells, we examined changes in their mRNA levels

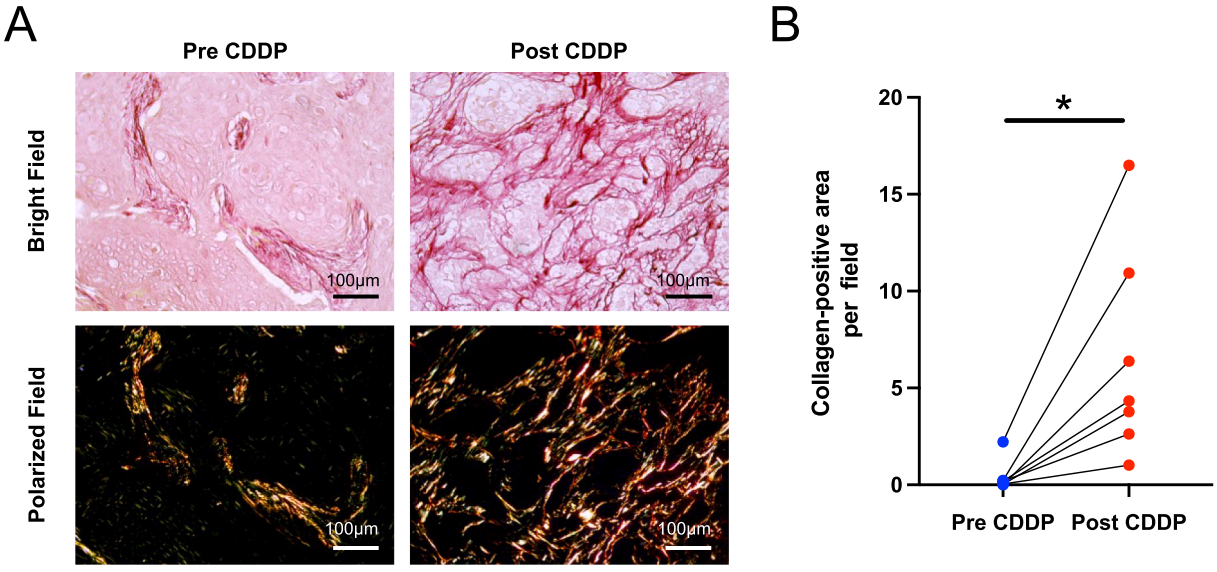

Fig. 1. Elevated collagen deposition in CDDP-treated surgically resected residual human OSCC tumors. (A) The residual human tumors (post-CDDP) and their matched biopsy tumors (pre-CDDP) were stained with Picro-Sirius Red (n = 7). Representative images captured by bright-field (parallel) and polarized light (orthogonal collagen) are shown. (B) Orthogonal collagen was measured as the percentage of total unmasked pixels except perivascular in the field of view at a final magnification of × 200. Scale bar indicates 100 μm. The graph depicted individual cases of orthogonal collagen pre- and post-treatment. Data were analyzed by the paired *t*-test, *p < 0.05.

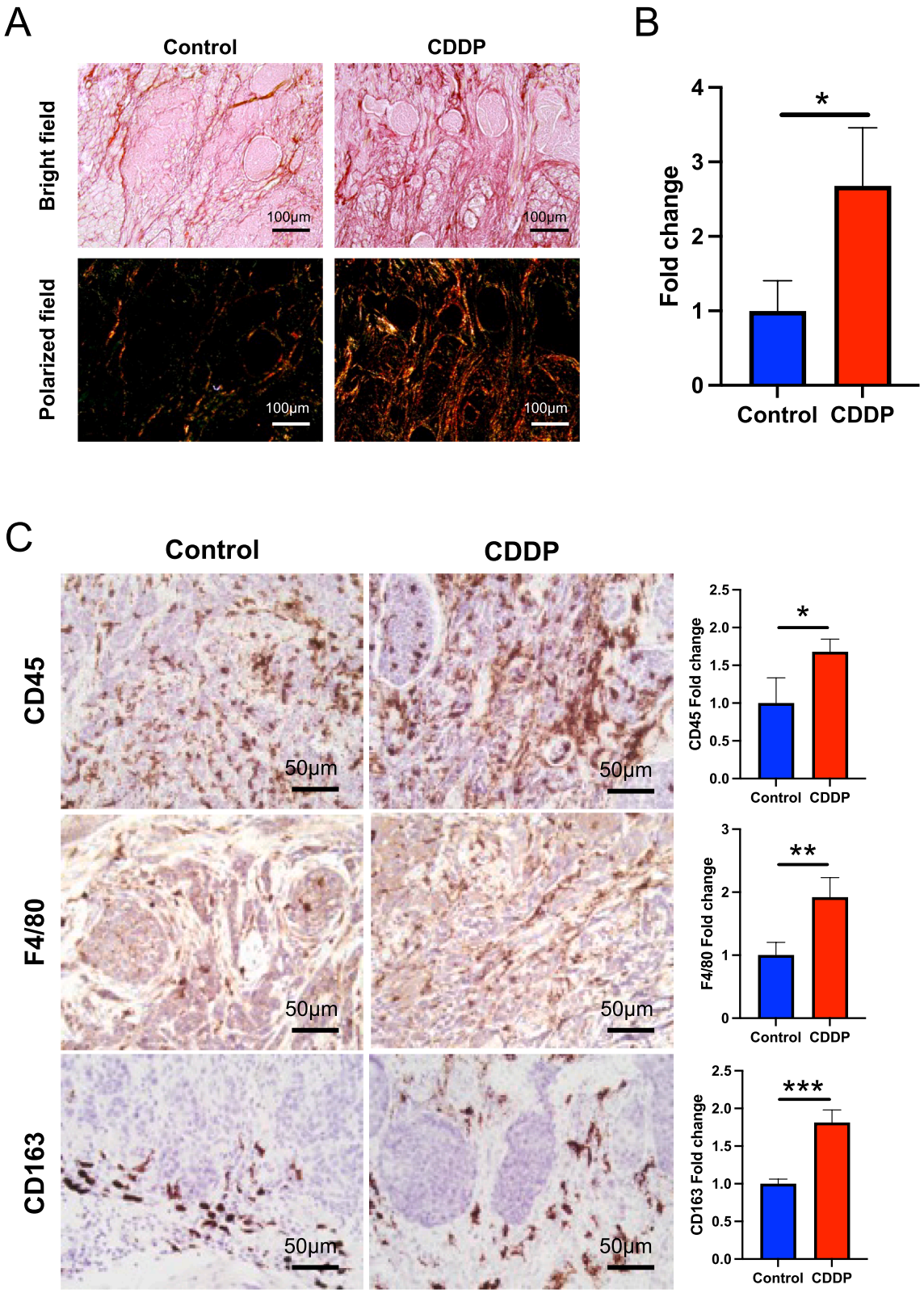

Fig. 2. CDDP-induced collagen deposition, leukemic cells, and macrophage change in mouse tumors. (A) The CDDP-treated mouse tumors (CDDP) and the non-treated mouse tumors (control) were stained with Picro-Sirius Red (n = 3). Representative images captured by bright-field (parallel) and polarized light (orthogonal collagen) are shown. (B) Orthogonal collagen was measured as the percentage of total unmasked pixels except perivascular in the field of view at a final magnification of × 200. Scale bar indicates 100 μm. The graph depicted the mean of orthogonal collagen as a multiple of the expression level in the control tumor group. Data were analyzed by the student *t*-test, *p < 0.05. (C) The number of Cd45-positive leukemic cells, F4/80-positive macrophages, and Cd163-positive M2-TAMs significantly increased in CDDP-treated tumors compared to non-treated tumors. Quantitative data are shown on the right. Five views were taken, and the mean positive cell count per view was calculated. Each tumor: n = 3; scale bar: 50 μm. *p < 0.05, **p < 0.01, ***p < 0.001.

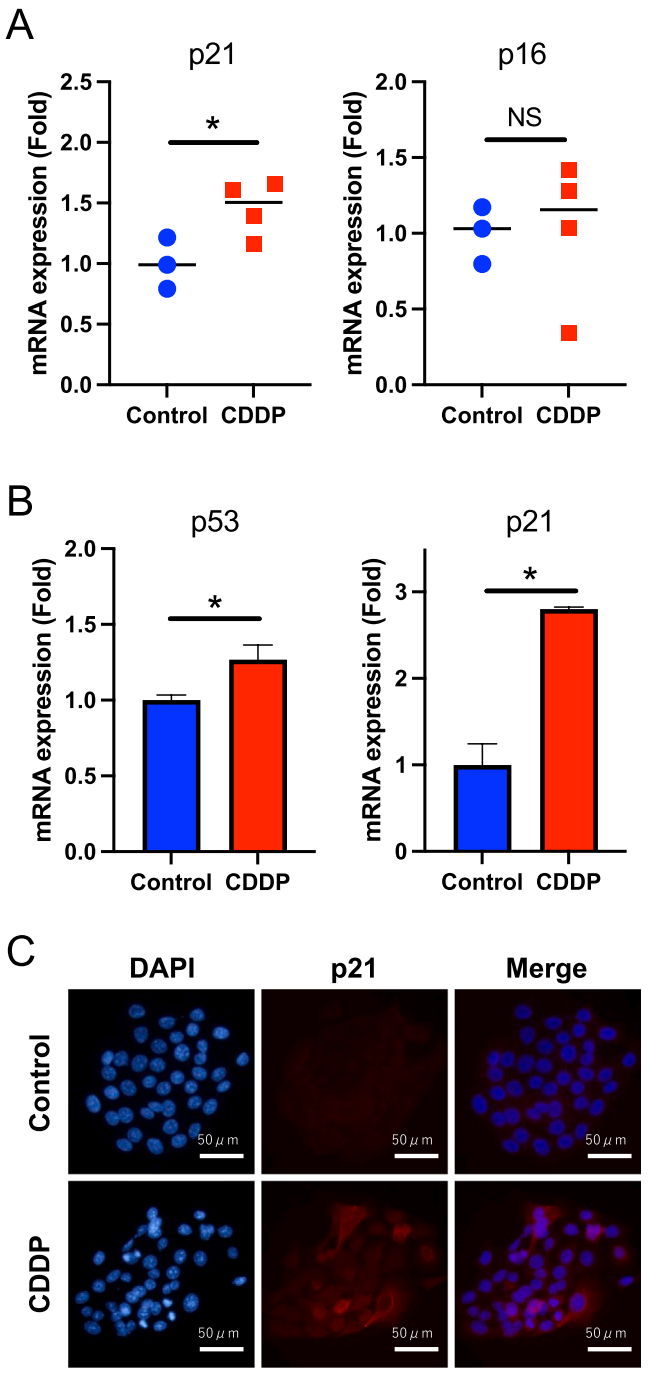

Fig. 3. Effect of CDDP treatment on cellular senescence of mouse tumor. (A) RNA extracted from CDDP-treated or non-treated tumor tissues was used to compare p21 and p16 mRNA expression levels within each tumor by RT-qPCR. mRNA expression levels are shown. The expression levels of each gene were corrected for Gapdh expression and expressed as a multiple of the expression level in the control tumor group. Values represent mean and standard deviation. Control group; n = 3, CDDP group; n = 4. *p < 0.05. (B) RNA extracted from CDDP-treated or non-treated tumor cells was used to compare p53 and p21 mRNA expression levels within each cell by RT-qPCR. mRNA expression levels are shown. The expression levels of each gene were corrected for Gapdh expression and expressed as a multiple of the expression level in the control group. Values represent mean and standard deviation. n = 3. *p < 0.05, ***p < 0.001. (C) Immunocytochemical staining of p21 protein is shown; protein expression of p21 increased in CDDP-treated tumor cells compared to non-treated cells. Red: p21 (middle); blue: DAPI. Scale bar: 50 μm.

by adding UC2288. The results showed that the addition of UC2288 significantly decreased the expression of IL-6, CXCL1, CCL2, CCL5, CXCL9, and IL-13 compared to that in cells treated with CDDP alone (Fig. 5C). These results suggest that CDDP-induced senescence of oral cancer cells induced by p21 expression promotes the secretion of SASP factors, such as CCL5.

3.6. Effect of p21 inhibitor on desmoplasia-like structural changes induced by CDDP administration in tongue tumor tissues of tumor-bearing mice

Finally, to examine whether CDDP-induced changes in the TME were related to SASP factors due to cellular senescence, we conducted an experiment in which CDDP and a p21 inhibitor were administered to a syngeneic transplant mouse model. Tongue tumors removed from tumor-bearing mice treated with CDDP and UC2288 were evaluated by Picrosirius Red staining. Picro-Sirius Red staining was performed to evaluate the collagen fibers. Under a bright-field microscope, bundles of collagen fibers were observed in the CDDP-treated group. However, the number of bundles decreased in the UC2288-treated group. Polarized light microscopy revealed that thick collagen fibers, depicted in yellow to orange, were significantly decreased in the UC2288-treated group compared to those in the CDDP-treated group (Fig. 6). These results suggest that CDDP administration-induced desmoplasia-like structural changes in the TME are related to cellular senescence.

4. Discussion

Desmoplasia, an increase in the fibrous ECM in the TME, is prominent in pancreatic cancer. Whatcott et al. reported that hyaluronic acid and collagen fibers, specifically in the ECM, are highly expressed in pancreatic cancer tissues compared with normal tissues [34]. Abundant hyaluronic acid and collagen fibers in tumor tissues can cause increased interstitial fluid pressure, rupture of blood vessels, and decreased vascular permeability, resulting in impaired drug delivery to tumor cells, suggesting resistance to drug therapy [35]. In addition, increased infiltration of immune cells and desmoplasia-like changes due to inflammation after drug therapy have been reported both in clinical specimens of breast cancer and esophageal squamous cell carcinoma and in mouse studies [31,36–38]. In this study, we observed a marked increase in collagen expression around the remaining tumor cells after CDDP administration in clinical specimens of oral cancer. We demonstrated for the first time that desmoplasia-like changes occurred. Additionally, in a mouse model, an increase in collagen was observed in the CDDP-treated group, and the researchers succeeded in reproducing the changes observed in clinical specimens.

Tumor cell remains after drug therapy or radiotherapy have been known to be one of the causes of local recurrence, lymph node metastasis, and distant metastasis in patients with OSCC [39]. The involvement of cancer cells remaining after drug therapy or radiotherapy in recurrence and metastasis has been reported in breast, prostate, and lung cancers [40–42]. Furthermore, cancer cells remaining after drug therapy or radiotherapy contain senescent cells caused by senescence [16,43–45]. In this study, we found an increase in the expression of p21, a marker for senescent cells, in the tumor tissue of tumor-bearing mice after administration of the anticancer drug CDDP; treatment of cultured oral cancer cells with CDDP showed that oral cancer cells increased expression of p21 and SASP factors indicated that senescence was likely induced in the remaining oral cancer cells after CDDP administration. Senescence in oral cancer cells was driven by increased p21 expression, with no concurrent increase in p16 expression observed. Ahmadinejad et al. also reported in a study using head and neck cancer cells that senescence in cancer cells is mediated by p21 [16]. Mirzayans et al. showed that the senescence of cancer cells caused by radiation therapy-induced stress is due to p21 in breast cancer cells without p53 mutations. In contrast, p16 is vital in breast cancer cells with p53 mutations [46].

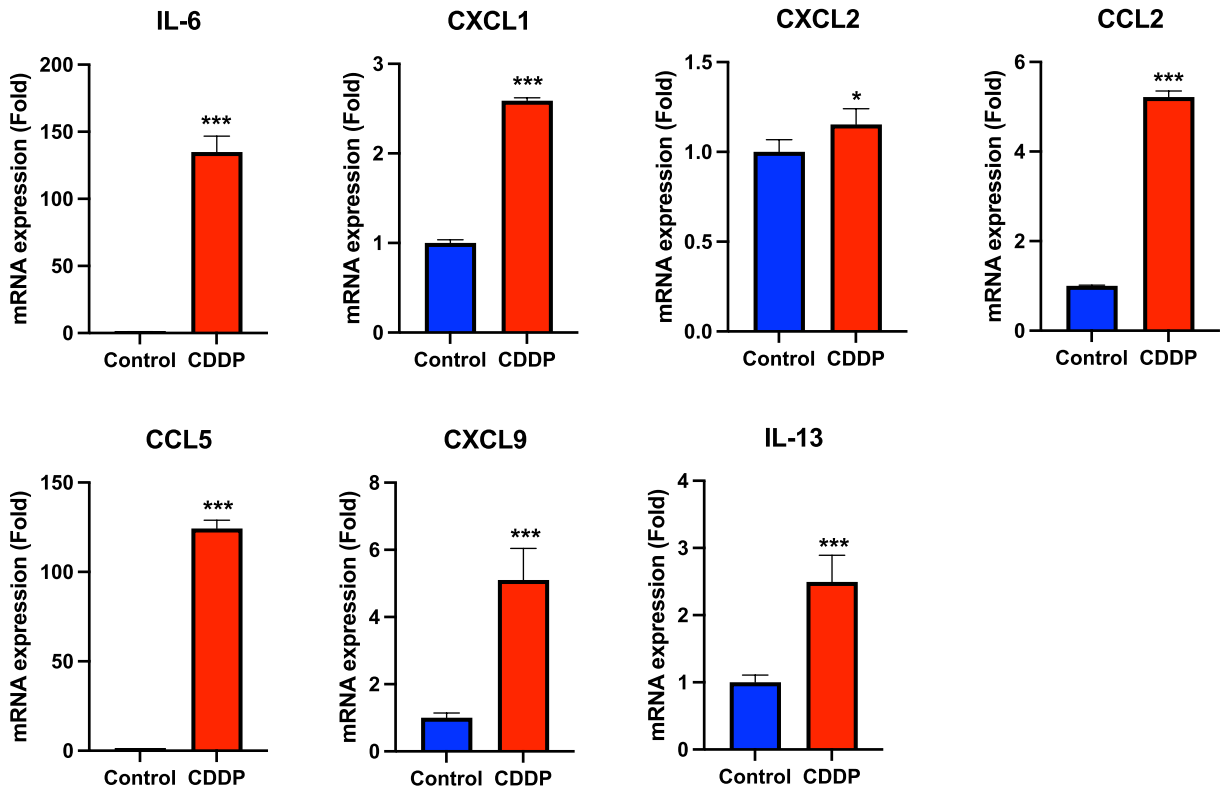

Fig. 4. Effect of CDDP treatment on the expression of SASP factors in mouse tumor cells. RNA extracted from CDDP-treated or non-treated tumor cells was used by RT-qPCR to compare mRNA expression levels of SASP factors within each cell. mRNA expression levels are shown. The expression levels of each gene were corrected for Gapdh expression and expressed as a multiple of the expression level in the control group. Values represent mean and standard deviation. n = 3. *p < 0.05, ***p < 0.001.

They pointed out that p21 may suppress p16 expression, which requires further investigation.

Although anticancer treatment-induced cellular senescence has been studied for decades, the involvement of senescent cancer cells in recurrence remains unclear [47]. Initially, cellular senescence was assumed to be an early response to drugs or radiotherapy. It was considered a favorable outcome of cancer treatment owing to its features, such as long-term growth arrest, which may lead to tumor shrinkage [48]. However, senescent cells in the remaining tumor tissue survive by maintaining a state of growth arrest because senescent cells are resistant to apoptosis. Senescent cells begin regaining from the surrounding quiescent cancer cells by secreting SASP factors [16,49–51]. Cancer cell regrowth is associated with interactions with the TME, such as CAF and TAM [41].

TAMs, the most frequently found immune cells in the TME, play an important role in mediating immune responses in cancers [52]. Macrophages change their dynamics and functions depending on their microenvironment, are classified into M1 and M2 types depending on their characteristics, and play anti-inflammatory and proinflammatory roles [53]. Many TAMs exhibit properties similar to M2 macrophages, and various ECM components are involved in the polarization of TAMs from M1 to M2 [54]. In particular, type I collagen has long been reported to be involved in the M2 polarization of TAMs [1,55,56]. Furthermore, the M1 type of TAM promotes cancer development, and the M2 type promotes cancer progression [57]. Morita et al. showed that administering anticancer drugs increased M2-TAM levels in mouse breast cancer tissues, leading to desmoplasia-like changes. Furthermore, they reported that reducing intratumoral M2-TAM by blocking E-selectin in vascular endothelial cells can suppress desmoplasia-like changes after chemotherapy, indirectly affecting the TME after drug therapy. They showed that M2-TAM plays an important role in desmoplasia-like changes in the human body [31]. In this study, CDDP administration to tumor-bearing mice increased the number of immune cells, M2-TAM, collagen fibers, and desmoplasia-like changes. This suggests that increased M2-TAM levels in the TME are involved in desmoplasia-like changes, similar to the results observed in breast cancer.

CCL2, also known as monocyte chemotactic protein 1 (MCP-1), is a 13 kDa protein consisting of 76 amino acids, and it is known that CCL2 has two cysteine residues adjacent to its amino terminus [33,58]. CCL2 regulates the migration and infiltration of various immune cells, including monocytes, macrophages, memory T lymphocytes, and natural killer (NK) cells [33,58,59]. CCL5 is a small 8 kDa chemokine that attracts T cells, macrophages, endothelial cells, and fibroblasts by binding to its receptor [60,61]. Furthermore, an increasing number of reports have demonstrated that CCL5 promotes tumor growth and metastasis by inducing TAM polarity to the M2 type [62–67]. For example, Mi et al. found that THP-1 macrophages co-cultured with CCL5 exhibited increased expression of M2-related genes [65]. Nieto et al. showed that CCL5 increases the expression of CD163 (a marker for M2-TAM) in human monocytes [63]. IL-13 is a classic and potent M2-TAM polarity-inducing cytokine [68–73]. In the present study, the mRNA expression levels of IL-6, CXCL1, CCL2, CCL5, CXCL9, and IL-13, which were increased by CDDP treatment, were reduced by adding a p21 inhibitor. IL-6, CXCL1, CCL2, CCL5, and CXCL9 have been previously reported as SASP factors [32,74]. In addition, IL-13 has been reported as an SASP factor in recent years [75]. In this study, IL-13 is possibly one of the SASP factors. Moreover, we suggest that in oral cancer, cell senescence occurs in the remaining cancer cells due to exposure to anticancer drugs. CCL2, secreted from senescent cells as an SASP factor, may induce macrophages near cancer cells. TAM is known to be M1-TAM in its early stages [57]. Hence, our results suggest that M1-TAM acquires M2 polarity through the SASP factors, CCL5 and IL-13. As an M2-TAM, it may have various effects on the TME, including desmoplasia-like changes (Fig. 7).

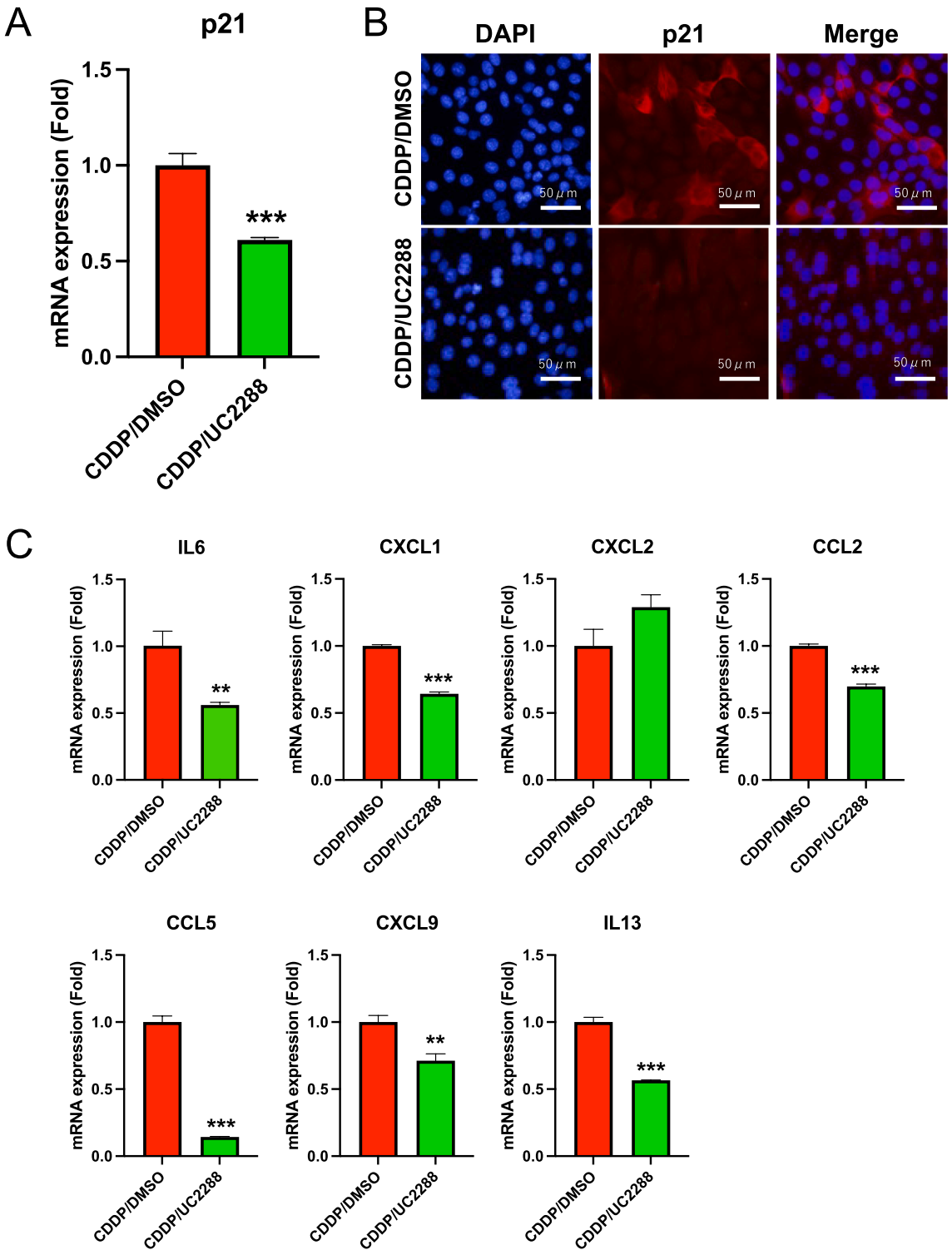

Fig. 5. Effect of p21 inhibitor on CDDP-induced cellular senescence in mouse tumor cells. (A) RNA extracted from CDDP-treated mouse tumor culture cells in the presence and absence of UC2288 was used to compare mRNA expression levels by RT-qPCR. mRNA expression levels are shown. The expression levels of each gene were corrected for Gapdh expression and expressed as a multiple of the expression level in the Pa cells group. Values represent mean and standard deviation. n = 3. ***p < 0.001. (B) Immunocytochemical staining of p21 protein in CDDP-treated tumor cells is shown; protein expression of p21 decreased in the presence of UC2288 compared to the absence. Red: p21 (middle); blue: DAPI. Scale bar: 50 μm. (C) RNA extracted from CDDP-treated tumor cells in the presence and absence of UC2288 was used to compare mRNA expression levels of SASP factors within each cell by RT-qPCR. mRNA expression levels are shown. The expression levels of each gene were corrected for Gapdh expression and expressed as a multiple of the expression level in the control group. Values represent mean and standard deviation. n = 3. **p < 0.01, ***p < 0.001.

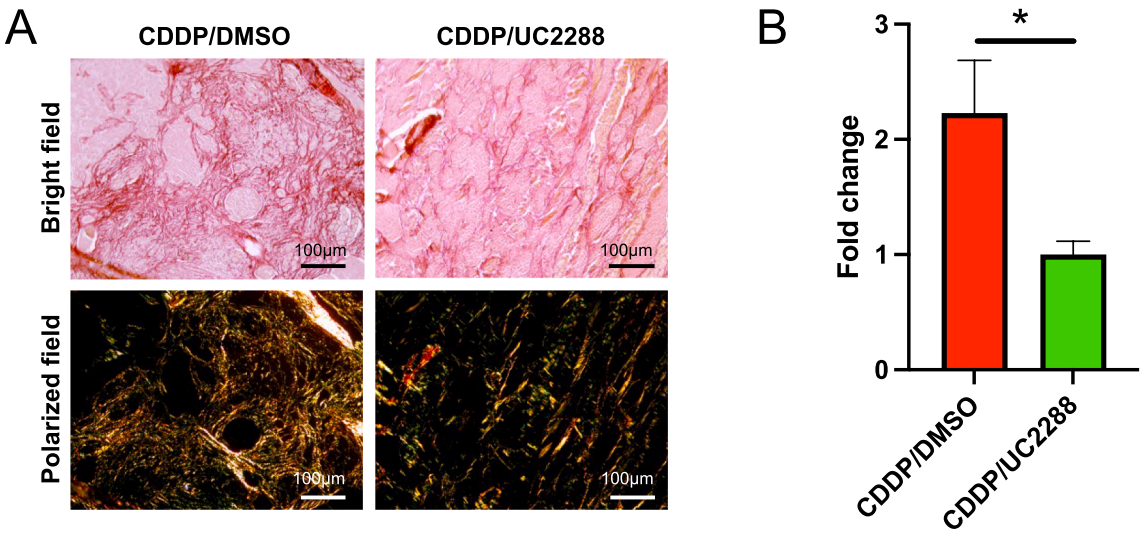

Fig. 6. Effect of p21 inhibitor for CDDP-induced collagen deposition change in mouse tumors. (A) The CDDP/UC2288-treated mouse tumors (CDDP/UC2288) and the CDDP/DMSO-treated mouse tumors (CDDP/DMSO) were stained with Picro-Sirius Red (n = 3). Representative images captured by bright-field (parallel) and polarized light (orthogonal collagen) microscopy are shown. (B) Orthogonal collagen was measured as the percentage of total unmasked pixels except perivascular in the field of view at a final magnification of × 200. Scale bar indicates 100 μm. The graph depicted the mean of orthogonal collagen as a multiple of the expression level in the CDDP/DMSO tumor group. Data were analyzed by the student *t*-test, *p < 0.05.

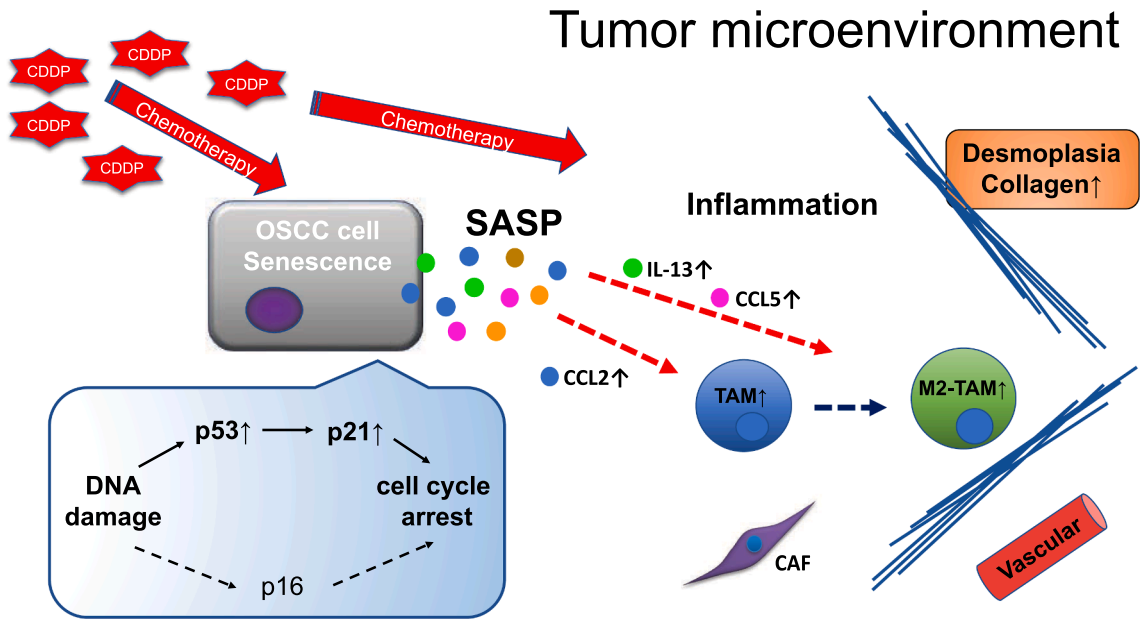

Fig. 7. Schematic model of the change of tumor microenvironment by CDDP-induced cell senescence. CDDP directly induces inflammation in the tumor microenvironment but, at the same time, induces cellular senescence in cancer cells, which releases SASP factors into the tumor microenvironment. Ultimately, these SASP factors lead to an increase in TAM within the tumor microenvironment, resulting in an increase in collagen, which is a desmoplasia-like change.

Although we have shown that inhibiting cancer cell senescence may suppress the changes in the TME caused by anticancer drugs, which are detrimental to cancer treatment, complete inhibition of cell senescence is challenging. To suppress aging, the development of senolytic drugs that specifically kill senescent cells and senomorphic drugs that act on the signal pathway of senescent cells, primarily reducing the secretion of SASP factors, are attracting attention. Demaria et al. reported that eliminating doxorubicin-induced senescent cells with a senolytic drug inhibited cancer recurrence and metastasis [17]. However, cellular senescence in living organisms has been shown to have anti-carcinogenic effects [76,77]. Therefore, understanding the dual nature of cellular senescence in cancer and appropriately controlling cellular senescence is vital.

5. Conclusions

This study showed that changes in the TME caused by anticancer drugs may be related to SASP factors, which are inflammatory cytokines secreted by cancer cells. Analysis of the TME is becoming increasingly important in cancer research; however, it cannot be performed using conventional immunodeficient mouse models. In this study, replicating in-vivo reactions observed upon administration of anticancer drugs to immunocompetent mice and subsequently analyzing these responses alongside clinical specimens may lead to the development of new treatment strategies to make anticancer drug treatment more effective.

CRediT authorship contribution statement

Junya Nishimura: Writing – review & editing, Writing – original draft, Visualization, Supervision, Software, Methodology, Investigation, Funding acquisition, Data curation, Conceptualization. **Yoshihiro Morita:** Writing – review & editing, Writing – original draft, Visualization, Validation, Supervision, Software, Resources, Methodology, Investigation, Funding acquisition, Formal analysis, Data curation, Conceptualization. **Ayano Tobe-Nishimoto:** Writing – review & editing, Visualization, Software, Methodology, Investigation. **Yukiko Kitahira:** Visualization, Software, Investigation. **Shun Takayama:** Validation, Methodology, Investigation. **Satoko Kishimoto:** Writing – review & editing, Validation, Methodology. **Yuka Matsumiya-Matsumoto:** Writing – review & editing, Validation, Methodology. **Akinori Takeshita:** Writing – review & editing, Validation, Methodology. **Kazuhide Matsunaga:** Writing – review & editing, Validation, Methodology. **Tomoaki Imai:** Writing – review & editing, Validation, Methodology, Formal analysis. **Narikazu Uzawa:** Writing – review & editing, Writing – original draft, Validation, Resources, Funding acquisition, Data curation, Conceptualization.

Declaration of competing interest

The authors declare that they have no known competing financial interests or personal relationships that could have appeared to influence the work reported in this paper.

Data availability

Data will be made available on request.

Acknowledgments

We would like to express our deepest gratitude to Associate Professor Ryoji Yoshida (Kumamoto University) and Dr. Koichi Ando (Gunma University) for providing us with cells.

We would like to thank Editage (www.editage.jp) for English language editing.

Institutional Review Board Statement: The animal experiments were approved by the Osaka University Graduate School of Dentistry Institutional Animal Use Committee (Approval number: R-01-004-0) and the clinical experiments were approved by the Osaka University Graduate School of Dentistry Research Ethics Committee (Approval number: H30-E50-1). All methods were performed in accordance with the relevant guidelines and regulations of the Basel Declaration. The study is reported in accordance with ARRIVE guidelines.

Funding

This work was supported by JSPS KAKENHI Grant Nos. JP18K09809, JP21K21085, JP23K19688, and JP19K21410, and by crowdfunding contributed through READYFOR.

Appendix A. Supplementary material

Supplementary data to this article can be found online at https://doi.org/10.1016/j.intimp.2024.112377.

References

[1] E. Henke, R. Nandigama, S. Ergün, Extracellular matrix in the tumor microenvironment and its impact on cancer therapy, Front. Mol. Biosci. 6 (2019) 160, https://doi.org/10.3389/fmolb.2019.00160.

[2] H. Hurwitz, L. Fehrenbacher, W. Novotny, T. Cartwright, J. Hainsworth, W. Heim, J. Berlin, A. Baron, S. Griffing, E. Holmgren, N. Ferrara, G. Fyfe, B. Rogers, R. Ross, F. Kabbinavar, Bevacizumab plus irinotecan, fluorouracil, and leucovorin for metastatic colorectal cancer, N. Engl. J. Med. 350 (2004) 2335–2342, https://doi.org/10.1056/NEJMoa032691.

[3] C. Robert, J. Schachter, G.V. Long, A. Arance, J.J. Grob, L. Mortier, A. Daud, M. S. Carlino, C. McNeil, M. Lotem, J. Larkin, P. Lorigan, B. Neyns, C.U. Blank, O. Hamid, C. Mateus, R. Shapira-Frommer, M. Kosh, H. Zhou, N. Ibrahim, S. Ebbinghaus, A. Ribas, Pembrolizumab versus ipilimumab in advanced melanoma, N. Engl. J. Med. 372 (2015) 2521–2532, https://doi.org/10.1056/NEJMoa1503093.

[4] T. Mammoto, A. Jiang, E. Jiang, D. Panigrahy, M.W. Kieran, A. Mammoto, Role of collagen matrix in tumor angiogenesis and glioblastoma multiforme progression, Am. J. Pathol. 183 (2013) 1293–1305, https://doi.org/10.1016/j.ajpath.2013.06.026.

[5] P.P. Provenzano, D.R. Inman, K.W. Eliceiri, J.G. Knittel, L. Yan, C.T. Rueden, J. G. White, P.J. Keely, Collagen density promotes mammary tumor initiation and progression, BMC Med. 6 (2008) 11, https://doi.org/10.1186/1741-7015-6-11.

[6] T. Casey, J. Bond, S. Tighe, T. Hunter, L. Lintault, O. Patel, J. Eneman, A. Crocker, J. White, J. Tessitore, M. Stanley, S. Harlow, D. Weaver, H. Muss, K. Plaut, Molecular signatures suggest a major role for stromal cells in development of invasive breast cancer, Breast Cancer Res. Treat 114 (2009) 47–62, https://doi.org/10.1007/s10549-008-9982-8.

[7] A. Naba, K.R. Clauser, S. Hoersch, H. Liu, S.A. Carr, R.O. Hynes, The matrisome: in silico definition and in vivo characterization by proteomics of normal and tumor extracellular matrices*, Mol. Cell. Proteom. 11 (2012) M111.014647. 10.1074/mcp.M111.014647.

[8] R. Afik, E. Zigmond, M. Vugman, M. Klepfish, E. Shimshoni, M. Pasmanik-Chor, A. Shenoy, E. Bassat, Z. Halpern, T. Geiger, I. Sagi, C. Varol, Tumor macrophages are pivotal constructors of tumor collagenous matrix, J. Exp. Med. 213 (2016) 2315–2331, https://doi.org/10.1084/jem.20151193.

[9] C. Deligne, K.S. Midwood, Macrophages and extracellular matrix in breast cancer: partners in crime or protective allies? Front. Oncol. 11 (2021) 620773 https://doi.org/10.3389/fonc.2021.620773.

[10] J.A. Conti, T.J. Kendall, A. Bateman, T.A. Armstrong, A. Papa-Adams, Q. Xu, G. Packham, J.N. Primrose, R.C. Benyon, J.P. Iredale, The desmoplastic reaction surrounding hepatic colorectal adenocarcinoma metastases aids tumour growth and survival via αv integrin ligation, Clin. Cancer Res. 14 (2008) 6405–6413, https://doi.org/10.1158/1078-0432.CCR-08-0816.

[11] M. Schober, R. Jesenofsky, R. Faissner, C. Weidenauer, W. Hagmann, P. Michl, R. Heuchel, S. Haas, J.-M. Löhr, Desmoplasia and chemoresistance in pancreatic cancer, Cancers 6 (2014) 2137–2154, https://doi.org/10.3390/cancers6042137.

[12] G.J.K. Guthrie, K.A. Charles, C.S.D. Roxburgh, P.G. Horgan, D.C. McMillan, S. J. Clarke, The systemic inflammation-based neutrophil-lymphocyte ratio: experience in patients with cancer, Crit. Rev. Oncol. Hematol. 88 (2013) 218–230, https://doi.org/10.1016/j.critrevonc.2013.03.010.

[13] D. Schaue, E.D. Micewicz, J.A. Ratikan, M.W. Xie, G. Cheng, W.H. McBride, Radiation and inflammation, Semin. Radiat. Oncol. 25 (2015) 4–10, https://doi.org/10.1016/j.semradonc.2014.07.007.

[14] J.A. Ewald, J.A. Desotelle, G. Wilding, D.F. Jarrard, Therapy-induced senescence in cancer, J. Natl. Cancer Inst. 102 (2010) 1536–1546, https://doi.org/10.1093/jnci/djq364.

[15] M. Schosserer, J. Grillari, M. Breitenbach, The dual role of cellular senescence in developing tumors and their response to cancer therapy, Front. Oncol. 7 (2017) 278, https://doi.org/10.3389/fonc.2017.00278.

[16] F. Ahmadinejad, T. Bos, B. Hu, E. Britt, J. Koblinski, A.J. Souers, J.D. Leverson, A. C. Faber, D.A. Gewirtz, H. Harada, Senolytic-mediated elimination of head and neck tumor cells induced into senescence by cisplatin, Mol. Pharmacol. 101 (2022) 168–180, https://doi.org/10.1124/molpharm.121.000354.

[17] M. Demaria, M.N. O'Leary, J. Chang, L. Shao, S. Liu, F. Alimirah, K. Koenig, C. Le, N. Mitin, A.M. Deal, S. Alston, E.C. Academia, S. Kilmarx, A. Valdovinos, B. Wang, A. de Bruin, B.K. Kennedy, S. Melov, D. Zhou, N.E. Sharpless, H. Muss, J. Campisi, Cellular senescence promotes adverse effects of chemotherapy and cancer relapse, Cancer Discov. 7 (2017) 165–176, https://doi.org/10.1158/2159-8290.CD-16-0241.

[18] C. Duy, M. Li, M. Teater, C. Meydan, F.E. Garrett-Bakelman, T.C. Lee, C.R. Chin, C. Durmaz, K.C. Kawabata, E. Dhimolea, C.S. Mitsiades, H. Doehner, R. J. D'Andrea, M.W. Becker, E.M. Paietta, C.E. Mason, M. Carroll, A.M. Melnick, Chemotherapy induces senescence-like resilient cells capable of initiating AML recurrence, Cancer Discov. 11 (2021) 1542–1561, https://doi.org/10.1158/2159-8290.CD-20-1375.

[19] V. Gorgoulis, P.D. Adams, A. Alimonti, D.C. Bennett, O. Bischof, C. Bishop, J. Campisi, M. Collado, K. Evangelou, G. Ferbeyre, J. Gil, E. Hara, V. Krizhanovsky, D. Jurk, A.B. Maier, M. Narita, L. Niedernhofer, J.F. Passos, P.D. Robbins, C. A. Schmitt, J. Sedivy, K. Vougas, T. von Zglinicki, D. Zhou, M. Serrano, M. Demaria, Cellular senescence: defining a path forward, Cell 179 (2019) 813–827, https://doi.org/10.1016/j.cell.2019.10.005.

[20] F. Rodier, J.-P. Coppé, C.K. Patil, W.A.M. Hoeijmakers, D.P. Muñoz, S.R. Raza, A. Freund, E. Campeau, A.R. Davalos, J. Campisi, Persistent DNA damage signalling triggers senescence-associated inflammatory cytokine secretion, Nat. Cell Biol. 11 (2009) 973–979, https://doi.org/10.1038/ncb1909.

[21] J.-P. Coppé, C.K. Patil, F. Rodier, Y. Sun, D.P. Muñoz, J. Goldstein, P.S. Nelson, P.-Y. Desprez, J. Campisi, Senescence-associated secretory phenotypes reveal cell-nonautonomous functions of oncogenic RAS and the p53 tumor suppressor, PLoS Biol. 6 (2008) e301.

[22] B. Wang, J. Kohli, M. Demaria, Senescent cells in cancer therapy: friends or foes? Trends in Cancer 6 (2020) 838–857, https://doi.org/10.1016/j.trecan.2020.05.004.

[23] J.G. Jackson, V. Pant, Q. Li, L.L. Chang, A. Quintás-Cardama, D. Garza, O. Tavana, P. Yang, T. Manshouri, Y. Li, A.K. El-Naggar, G. Lozano, p53-Mediated senescence impairs the apoptotic response to chemotherapy and clinical outcome in breast cancer, Cancer Cell 21 (2012) 793–806, https://doi.org/10.1016/j.ccr.2012.04.027.

[24] H. Sung, J. Ferlay, R.L. Siegel, M. Laversanne, I. Soerjomataram, A. Jemal, F. Bray, Global Cancer Statistics 2020: GLOBOCAN estimates of incidence and mortality worldwide for 36 cancers in 185 countries, CA: A, Cancer J. Clin. 71 (2021) 209–249, https://doi.org/10.3322/caac.21660.

[25] K. Muraoka, K. Okumura, H. Kitajo, H. Kato, M. Arisue, Chemokine receptor expression in oral squamous cell carcinoma: correlation with growth factor- and cytokine-mediated cell migration in vitro, Oral Sci. Int. 4 (2007) 73–85, https://doi.org/10.1016/S1348-8643(07)80002-4.

[26] K.D. Hunter, E.K. Parkinson, P.R. Harrison, Profiling early head and neck cancer, Nat. Rev. Cancer 5 (2005) 127–135.

[27] S. Takayama, Y. Morita, A. Nishimoto, J. Nishimura, K. Takebe, S. Kishimoto, Y. Matsumiya-Matsumoto, K. Matsunaga, T. Imai, N. Uzawa, GATA6 regulates expression of annexin A10 (ANXA10) associated with epithelial–mesenchymal transition of oral squamous cell carcinoma, Arch. Oral Biol. 144 (2022) 105569, https://doi.org/10.1016/j.archoralbio.2022.105569.

[28] D.J. Adelstein, Y. Li, G.L. Adams, H. Wagner, J.A. Kish, J.F. Ensley, D.E. Schuller, A.A. Forastiere, An intergroup phase III comparison of standard radiation therapy and two schedules of concurrent chemoradiotherapy in patients with unresectable squamous cell head and neck cancer, JCO 21 (2003) 92–98, https://doi.org/10.1200/JCO.2003.01.008.

[29] Y. Ota, T. Noguchi, E. Ariji, C. Fushimi, N. Fuwa, H. Harada, T. Hayashi, R. Hayashi, Y. Honma, M. Miura, T. Mori, H. Nagatsuka, M. Okura, M. Ueda, N. Uzawa, K. Yagihara, H. Yagishita, M. Yamashiro, S. Yanamoto, T. Kirita, J.S. of O. O. Scientific Committee on General Rules for Clinical and Pathological Studies of Oral Cancer, General rules for clinical and pathological studies on oral cancer (2nd edition): a synopsis, Int. J. Clin. Oncol. 26 (2021) 623–635. 10.1007/s10147-020-01812-9.

[30] K. Sakuma, T. Kii, H. Takahashi, S. Suzuki, K. Yoshikawa, T. Ogawa, A. Tanaka, An in vivo study of local administration of low-dose anti-PD-1 antibody using an oral cancer cell line, Anticancer Res. 42 (2022) 4293–4303, https://doi.org/10.21873/anticanres.15929.

[31] Y. Morita, M. Leslie, H. Kameyama, G.L.R. Lokesh, N. Ichimura, R. Davis, N. Hills, N. Hasan, R. Zhang, Y. Kondo, D.G. Gorenstein, D.E. Volk, I. Chervoneva, H. Rui, T. Tanaka, Functional blockade of e-selectin in tumor-associated vessels enhances anti-tumor effect of doxorubicin in breast cancer, Cancers 12 (2020) 725, https://doi.org/10.3390/cancers12030725.

[32] D.V. Faget, Q. Ren, S.A. Stewart, Unmasking senescence: context-dependent effects of SASP in cancer, Nat. Rev. Cancer 19 (2019) 439–453, https://doi.org/10.1038/s41568-019-0156-2.

[33] H. Zhang, K. Yang, F. Chen, Q. Liu, J. Ni, W. Cao, Y. Hua, F. He, Z. Liu, L. Li, G. Fan, Role of the CCL2-CCR2 axis in cardiovascular disease: Pathogenesis and clinical implications, Front. Immunol. 13 (2022) 975367, https://doi.org/10.3389/fimmu.2022.975367.

[34] C.J. Whatcott, C.H. Diep, P. Jiang, A. Watanabe, J. LoBello, C. Sima, G. Hostetter, H.M. Shepard, D.D. Von Hoff, H. Han, Desmoplasia in primary tumors and metastatic lesions of pancreatic cancer, Clin. Cancer Res. 21 (2015) 3561–3568, https://doi.org/10.1158/1078-0432.CCR-14-1051.

[35] N. Sato, S. Kohi, K. Hirata, M. Goggins, Role of hyaluronan in pancreatic cancer biology and therapy: once again in the spotlight, Cancer Sci. 107 (2016) 569–575, https://doi.org/10.1111/cas.12913.

[36] D.G. DeNardo, D.J. Brennan, E. Rexhepaj, B. Ruffell, S.L. Shiao, S.F. Madden, W. M. Gallagher, N. Wadhwani, S.D. Keil, S.A. Junaid, H.S. Rugo, E.S. Hwang, K. Jirström, B.L. West, L.M. Coussens, Leukocyte complexity predicts breast cancer survival and functionally regulates response to chemotherapy, Cancer Discov. 1 (2011) 54–67, https://doi.org/10.1158/2159-8274.CD-10-0028.

[37] J.D. Predina, B. Judy, L.A. Aliperti, Z.G. Fridlender, A. Blouin, V. Kapoor, B. Laguna, H. Nakagawa, A.K. Rustgi, L. Aguilar, E. Aguilar-Cordova, S.M. Albelda, S. Singhal, Neoadjuvant in situ gene-mediated cytotoxic immunotherapy improves postoperative outcomes in novel syngeneic esophageal carcinoma models, Cancer Gene Ther 18 (2011) 871–883, https://doi.org/10.1038/cgt.2011.56.

[38] T. Tsuchikawa, M.M. MD, Y. Yamamura, T. Shichinohe, S. Hirano, S. Kondo, The immunological impact of neoadjuvant chemotherapy on the tumor microenvironment of esophageal squamous cell carcinoma, Ann. Surg. Oncol. 19 (2012) 1713–1719. 10.1245/s10434-011-1906-x.

[39] M. Lambrecht, P. Dirix, W. Van den Bogaert, S. Nuyts, Incidence of isolated regional recurrence after definitive (chemo-) radiotherapy for head and neck squamous cell carcinoma, Radiother. Oncol. 93 (2009) 498–502, https://doi.org/10.1016/j.radonc.2009.08.038.

[40] T.M. Morgan, P.H. Lange, M.P. Porter, D.W. Lin, W.J. Ellis, I.S. Gallaher, R. L. Vessella, Disseminated tumor cells in prostate cancer patients after radical prostatectomy and without evidence of disease predicts biochemical recurrence, Clin. Cancer Res. 15 (2009) 677–683, https://doi.org/10.1158/1078-0432.CCR-08-1754.

[41] A. Walens, A.V. DiMarco, R. Lupo, B.R. Kroger, J.S. Damrauer, J.V. Alvarez, CCL5 promotes breast cancer recurrence through macrophage recruitment in residual tumors, Elife 8 (2019) e43653.

[42] C.-Y. Wu, C.-L. Lee, C.-F. Wu, J.-Y. Fu, C.-T. Yang, C.-T. Wen, Y.-H. Liu, H.-P. Liu, J.-C.-H. Hsieh, Circulating tumor cells as a tool of minimal residual disease can predict lung cancer recurrence: a longitudinal, prospective trial, Diagnostics (basel) 10 (2020) 144, https://doi.org/10.3390/diagnostics10030144.

[43] R.S. Kim, A. Avivar-Valderas, Y. Estrada, P. Bragado, M.S. Sosa, J.A. Aguirre-Ghiso, J.E. Segall, Dormancy signatures and metastasis in estrogen receptor positive and negative breast cancer, PLoS One 7 (2012) e35569.

[44] L.T.H. Phi, I.N. Sari, Y.-G. Yang, S.-H. Lee, N. Jun, K.S. Kim, Y.K. Lee, H.Y. Kwon, Cancer Stem Cells (CSCs) in drug resistance and their therapeutic implications in cancer treatment, Stem Cells Int. 2018 (2018) 5416923, https://doi.org/10.1155/2018/5416923.

[45] H. Wang, N.H. Stoecklein, P.P. Lin, O. Gires, Circulating and disseminated tumor cells: diagnostic tools and therapeutic targets in motion, Oncotarget 8 (2016) 1884–1912, https://doi.org/10.18632/oncotarget.12242.

[46] R. Mirzayans, B. Andrais, G. Hansen, D. Murray, Role of p16INK4A in replicative senescence and DNA damage-induced premature senescence in p53-deficient human cells, Biochem. Res. Int. 2012 (2012) 951574, https://doi.org/10.1155/2012/951574.

[47] P.A. Pérez-Mancera, A.R.J. Young, M. Narita, Inside and out: the activities of senescence in cancer, Nat. Rev. Cancer 14 (2014) 547–558, https://doi.org/10.1038/nrc3773.

[48] C. Nardella, J.G. Clohessy, A. Alimonti, P.P. Pandolfi, Pro-senescence therapy for cancer treatment, Nat. Rev. Cancer 11 (2011) 503–511, https://doi.org/10.1038/nrc3057.

[49] A. Seluanov, V. Gorbunova, A. Falcovitz, A. Sigal, M. Milyavsky, I. Zurer, G. Shohat, N. Goldfinger, V. Rotter, Change of the death pathway in senescent human fibroblasts in response to DNA damage is caused by an inability to stabilize p53, Mol. Cell Biol. 21 (2001) 1552–1564, https://doi.org/10.1128/MCB.21.5.1552-1564.2001.

[50] C.D. Wiley, J.M. Flynn, C. Morrissey, R. Lebofsky, J. Shuga, X. Dong, M.A. Unger, J. Vijg, S. Melov, J. Campisi, Analysis of individual cells identifies cell-to-cell variability following induction of cellular senescence, Aging Cell 16 (2017) 1043–1050, https://doi.org/10.1111/acel.12632.

[51] A. Hernandez-Segura, T.V. de Jong, S. Melov, V. Guryev, J. Campisi, M. Demaria, Unmasking transcriptional heterogeneity in senescent cells, Curr. Biol. 27 (2017) 2652–2660.e4, https://doi.org/10.1016/j.cub.2017.07.033.

[52] C.E. Lewis, J.W. Pollard, Distinct role of macrophages in different tumor microenvironments, Cancer Res. 66 (2006) 605–612, https://doi.org/10.1158/0008-5472.CAN-05-4005.

[53] M. Tariq, J. Zhang, G. Liang, L. Ding, Q. He, B. Yang, Macrophage polarization: anti-cancer strategies to target tumor-associated macrophage in breast cancer, J. Cell. Biochem. 118 (2017) 2484–2501, https://doi.org/10.1002/jcb.25895.

[54] H. Kim, J. Cha, M. Jang, P. Kim, Hyaluronic acid-based extracellular matrix triggers spontaneous M2-like polarity of monocyte/macrophage, Biomater. Sci. 7 (2019) 2264–2271, https://doi.org/10.1039/C9BM00155G.

[55] G. Kaplan, In vitro differentiation of human monocytes,monocytes cultured on glass are cytotoxic to tumor cells but monocytes cultured on collagen are not, J. Exp. Med. 157 (1983) 2061–2072, https://doi.org/10.1084/jem.157.6.2061.

[56] R.B. Wesley, X. Meng, D. Godin, Z.S. Galis, Extracellular matrix modulates macrophage functions characteristic to atheroma: collagen type I enhances acquisition of resident macrophage traits by human peripheral blood monocytes in vitro, Arterioscler. Thromb. Vasc. Biol. 18 (1998) 432–440, https://doi.org/10.1161/01.atv.18.3.432.

[57] A. Salmaninejad, S.F. Valilou, A. Soltani, S. Ahmadi, Y.J. Abarghan, R. J. Rosengren, A. Sahebkar, Tumor-associated macrophages: role in cancer development and therapeutic implications, Cell Oncol. (dordr.) 42 (2019) 591–608, https://doi.org/10.1007/s13402-019-00453-z.

[58] S.L. Deshmane, S. Kremlev, S. Amini, B.E. Sawaya, Monocyte Chemoattractant Protein-1 (MCP-1): An Overview, J. Interferon. Cytokine Res. 29 (2009) 313–326, https://doi.org/10.1089/jir.2008.0027.

[59] M. Singh, L. Cowell, S. Seo, G. O'Neill, E. Golemis, Molecular basis for HEF1/NEDD9/Cas-L action as a multifunctional co-ordinator of invasion, apoptosis and cell cycle, Cell Biochem. Biophys. 48 (2007) 54–72.

[60] R.E. Marques, R. Guabiraba, R.C. Russo, M.M. Teixeira, Targeting CCL5 in inflammation, Exp. Opin. Ther. Targets 17 (2013) 1439–1460, https://doi.org/10.1517/14728222.2013.837886.

[61] L. Shen, Y. Chen, J. Cheng, S. Yuan, S. Zhou, W. Yan, J. Liu, A. Luo, S. Wang, CCL5 secreted by senescent theca-interstitial cells inhibits preantral follicular development via granulosa cellular apoptosis, J. Cell. Physiol. 234 (2019) 22554–22564, https://doi.org/10.1002/jcp.28819.

[62] Y. Zhuang, X. Zhao, B. Yuan, Z. Zeng, Y. Chen, Blocking the CCL5–CCR5 Axis Using Maraviroc Promotes M1 polarization of macrophages cocultured with irradiated hepatoma cells, JHC 8 (2021) 599–611, https://doi.org/10.2147/JHC.S300165.

[63] J.C. Nieto, C. Zamora, E. Cantó, E. Garcia-Planella, J. Gordillo, M.A. Ortiz, C. Juárez, S. Vidal, CSF-1 regulates the function of monocytes in Crohn's disease patients in remission, Sci. Rep. 7 (2017) 92, https://doi.org/10.1038/s41598-017-00145-4.

[64] N. Halama, I. Zoernig, A. Berthel, C. Kahlert, F. Klupp, M. Suarez-Carmona, T. Suetterlin, K. Brand, J. Krauss, F. Lasitschka, T. Lerchl, C. Luckner-Minden, A. Ulrich, M. Koch, J. Weitz, M. Schneider, M.W. Buechler, L. Zitvogel, T. Herrmann, A. Benner, C. Kunz, S. Luecke, C. Springfeld, N. Grabe, C.S. Falk, D. Jaeger, tumoral immune cell exploitation in colorectal cancer metastases can be targeted effectively by anti-CCR5 therapy in cancer patients, Cancer Cell 29 (2016) 587–601, https://doi.org/10.1016/j.ccell.2016.03.005.

[65] S. Mi, Y. Qu, X. Chen, Z. Wen, P. Chen, Y. Cheng, Radiotherapy Increases 12-LOX and CCL5 Levels in esophageal cancer cells and promotes cancer metastasis via THP-1-derived macrophages, Onco Targets Ther 13 (2020) 7719–7733, https://doi.org/10.2147/OTT.S257852.

[66] Y. Ban, J. Mai, X. Li, M. Mitchell-Flack, T. Zhang, L. Zhang, L. Chouchane, M. Ferrari, H. Shen, X. Ma, Targeting Autocrine CCL5-CCR5 axis reprograms

immunosuppressive myeloid cells and reinvigorates antitumor immunity, Cancer Res. 77 (2017) 2857–2868, https://doi.org/10.1158/0008-5472.CAN-16-2913.
[67] Y. Nie, H. Huang, M. Guo, J. Chen, W. Wu, W. Li, X. Xu, X. Lin, W. Fu, Y. Yao, F. Zheng, M.-L. Luo, P.E. Saw, H. Yao, E. Song, H. Hu, Breast Phyllodes Tumors Recruit and Repolarize Tumor-Associated Macrophages via Secreting CCL5 to promote malignant progression, which can be inhibited by CCR5 Inhibition Therapy, Clin. Cancer Res. 25 (2019) 3873–3886, https://doi.org/10.1158/1078-0432.CCR-18-3421.
[68] S. Gao, J. Zhou, N. Liu, L. Wang, Q. Gao, Y. Wu, Q. Zhao, P. Liu, S. Wang, Y. Liu, N. Guo, Y. Shen, Y. Wu, Z. Yuan, Curcumin induces M2 macrophage polarization by secretion IL-4 and/or IL-13, J. Mol. Cell Cardiol. 85 (2015) 131–139, https://doi.org/10.1016/j.yjmcc.2015.04.025.
[69] S. Gordon, F.O. Martinez, Alternative activation of macrophages: mechanism and functions, Immunity 32 (2010) 593–604, https://doi.org/10.1016/j.immuni.2010.05.007.
[70] A. Mantovani, A. Sica, S. Sozzani, P. Allavena, A. Vecchi, M. Locati, The chemokine system in diverse forms of macrophage activation and polarization, Trends Immunol. 25 (2004) 677–686, https://doi.org/10.1016/j.it.2004.09.015.
[71] D.M. Mosser, J.P. Edwards, Exploring the full spectrum of macrophage activation, Nat. Rev. Immunol. 8 (2008) 958–969, https://doi.org/10.1038/nri2448.
[72] A. Sica, A. Mantovani, Macrophage plasticity and polarization: in vivo veritas, J. Clin. Invest. 122 (2012) 787–795, https://doi.org/10.1172/JCI59643.
[73] R.D. Stout, C. Jiang, B. Matta, I. Tietzel, S.K. Watkins, J. Suttles, Macrophages sequentially change their functional phenotype in response to changes in microenvironmental influences, J. Immunol. 175 (2005) 342–349, https://doi.org/10.4049/jimmunol.175.1.342.
[74] S. Kobashigawa, Y.M. Sakaguchi, S. Masunaga, E. Mori, Stress-induced cellular senescence contributes to chronic inflammation and cancer progression, Thermal Med. 35 (2019) 41–58, https://doi.org/10.3191/thermalmed.35.41.
[75] M. Zhu, S. Min, X. Mao, Y. Zhou, Y. Zhang, W. Li, L. Li, L. Wu, X. Cong, G. Yu, Interleukin-13 promotes cellular senescence through inducing mitochondrial dysfunction in IgG4-related sialadenitis, Int. J. Oral Sci. 14 (2022) 1–13, https://doi.org/10.1038/s41368-022-00180-6.
[76] M. Serrano, A.W. Lin, M.E. McCurrach, D. Beach, S.W. Lowe, Oncogenic ras provokes premature cell senescence associated with accumulation of p53 and p16INK4a, Cell 88 (1997) 593–602, https://doi.org/10.1016/S0092-8674(00)81902-9.
[77] F. Triana-Martínez, M.I. Loza, E. Domínguez, Beyond tumor suppression: senescence in cancer stemness and tumor dormancy, Cells 9 (2020) 346, https://doi.org/10.3390/cells9020346.